IUST International Journal of Engineering Science, Vol. 17, No.3-4, 2006, Page 47-52

Modeling of Heat Losses Within Combustion Chamber of Diesel Engines

M. Nikian, M. Naghashzadegan and S. K. Arya

Abstract: The cylinder working fluid mean temperature, rate of heat fluxes to combustion chamber and temperature distribution on combustion chamber surface will be calculated in this research. By simulating thermodynamic cycle of engine, temperature distribution of combustion chamber will be calculated by the Crank-Nicolson method. An implicit finite difference method was used in this code. Special treatments for piston movement and a grid transformation for describing the realistic piston bowl shape were designed and utilized. The results were compared with a finite element method and were verified to be accurate for simplified test problems. In addition, the method was applied to realistic problems of heat transfer in an Isuzu Diesel engine, and gave good agreement with available experimental.

Keywords: Heat loss, Combustion chamber, Diesel engine, Engine performance.

1. Introduction

It is known that heat transfer effects internal combustion engine performance, efficiency, and emissions. As far as performance is concerned, cooling for the cylinder head, cylinder wall, and piston is desired.

This is because of problems such as thermal stresses in regions of high heat flux, deterioration of the lubricating oil film, and knock and pre-ignition in spark ignition engines.

On the other hand, an increase of heat transfer to the combustion chamber walls will lower the gas temperature and pressure within the cylinder, which reduces the work per cycle transferred to the piston. Heat transfer from the working gas to the cooling system of a conventional Diesel engine accounts for up to 30% of the fuel energy. About 50% of this energy is lost through the piston and 30% through the head [1].

By simulating the thermodynamic cycle of engine, mean temperature of cylinder working fluid and heat fluxes to combustion chamber will be calculated.

Following that, using the heat conduction equations, by considering material property data and appropriate boundary conditions a temperature distribution is obtained for calculated heat fluxes.

The chamber wall temperature Tw is a vital parameter for determining magnitude of heat flux and engine cycle simulation. In general, cylinder wall, head and piston form the combustion chamber of an internal combustion engine, where the temperature distributions are different for each surface.

Typically, the temperature of each surface is assumed to be a constant [2] where this is not consistent with the actual situation occurring on the surface of the combustion.

2. Engine and Operating Specifications

The engine studied in this work was an Isuzu Diesel engine developed by Isuzu Ceramics Research Institute (ICRI). It is a ceramic, single cylinder DI Diesel engine. The piston crown, head, linear, cylinder and valves are made of Silicon Nitride (Kyocera SN235). This material has the following properties at room temperature: density $\rho = 3240\,\mathrm{kgm}^{-3}$;thermal conductivity k=31 $\mathrm{Wm}^{-1}\mathrm{K}^{-1}$; and specific heat cp=680 $\mathrm{Jkg}^{-1}\mathrm{K}^{-1}$. Additional insulation is provided by air gaps and insulating rings between the ceramics and the metal components of the engine.

The engine has limited cooling of the cylinder wall and of the bottom of the metal skirt of the piston.

Both of these regions are cooled by lubricating oil. The engine specification and operation conditions are listed in Table 1.

The primary feature used in the development of this cycle simulation is the first law of thermodynamics which is utilized to derive an expression for the crank angle (time) derivative of the overall gas temperature in terms of engine design variables, operating conditions, and sub-model parameters.

Paper first received August, 24, 2003 and in revised: Aug, 30, 2006.

M. Nikian is with the Department of Mechanical Engineering, Islamic Azad University of Takestan, m_nikian@hotmail.com.

M. Naghashzadegan is with the Department of Mechanical Engineering, University of Guilan.

S. K. Arya is with the Department of Mechanical Engineering, University of Uromia.

Table. 1. Specifications of Isuzu ceramic Diesel engine

Bore of cylinder	84	mm
Stroke	92	mm
Squish	1.3	mm
Compression ratio	12.6	—
Connecting rod	193	mm
Piston crown	shallow dish	—
Engine speed	1500	rev/min

3. Thermodynamic Cycle Simulation

The first law of thermodynamics for the one-zone formulation for this system is [3]:

$$\frac{dE}{d\theta} = \frac{dQ_{tot}}{d\theta} - \frac{dW}{d\theta} + \dot{m}_{in} h_{in} - \dot{m}_{out} h_{out} \qquad (1)$$

where E is the total energy, Q_{tot} is the total net heat input, W is the net work done by the system, $\dot{m}$ is the mass flow rate into or out of the system, and h is the specific enthalpy either into or out of the system.

The only significant energy of the system is internal energy (u), the only significant work term is due to the piston motion (system boundary motion). So equation (1) becomes:

$$\frac{d(mu)}{d\theta} = \dot{Q}_{tot} - p\dot{V} + \dot{m}_{in} h_{in} - \dot{m}_{out} h_{out} \qquad (2)$$

where m is the mass in the cylinder, p is the cylinder pressure, and $\dot{V}$ is the cylinder volume time rate of change.

To obtain a derivative of the pressure, which is independent of the gas temperature, an expression for the derivative of the pressure, $\dot{p}$ is needed. This may be obtained from the derivative of ideal gas equation of state:

$$\dot{p} = (mR\dot{T} + m\dot{R}T + \dot{m}RT - p\dot{V}) / V \qquad (3)$$

Combining equations (2), (3) and assuming that the composition and thermodynamic properties are constant therefore:

$$\dot{T} = \frac{1}{mC_v}(\dot{Q}_{tot} - p\dot{V} + \dot{m}_{in} C_p T_{in} - \dot{m}_{out} C_p T_{out} - u\dot{m}) \qquad (4)$$

and

$$\dot{p} = \frac{(\gamma - 1)}{V}\left\{\dot{Q}_{tot} - \left(\frac{\gamma}{\gamma - 1}\right)p\dot{V} + \dot{m}_{in} C_p T_{in} - \dot{m}_{out} C_p T_{out}\right\} \qquad (5)$$

Solving these differential equations and assuming a constant wall temperature the cylinder working fluid mean temperature, pressure and magnitude of heat fluxes to combustion chamber will be obtained.

Figures (1) and (2) show the pressure and gas temperature of cylinder working fluid against crank angle (time).

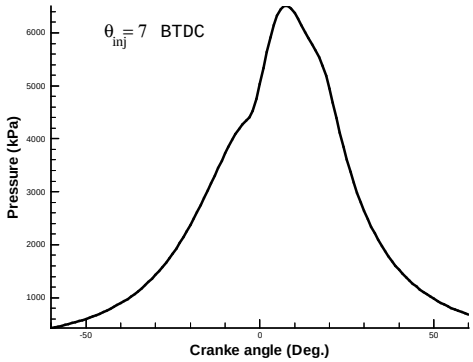

Fig. 1. Cylinder Pressure Against Crank Angle for Isuzu Engine

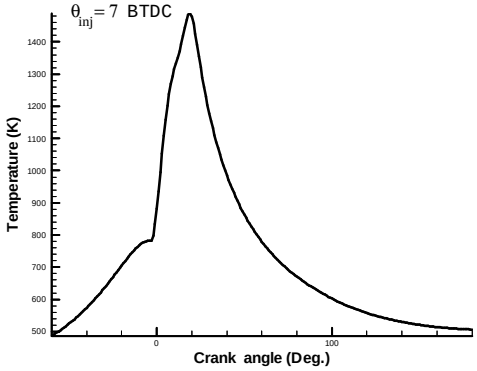

Fig. 2. Cylinder Temperature Against Crank Angle for Isuzu Engine

4. Models and Numerical Methods

The approach to determine the combustion chamber temperature distribution is deduced from the energy conservation law. For simplicity it is assumed that the engine geometry is axisymmetric. In two dimensional cylindrical coordinate the heat conduction equation is:

$$\frac{1}{r}\frac{\partial}{\partial r}\left(kr\frac{\partial T}{\partial r}\right) + \frac{\partial}{\partial r}\left(k\frac{\partial T}{\partial z}\right) = \rho c_p \frac{\partial T}{\partial t} \qquad (6)$$

where r and z are the coordinates in the radial and axial directions, respectively; T is the wall temperature; k is the thermal conductivity ; c_p is the specific heat and t is time.

As the boundary condition, the temperatures on the outer surface of the cylinder wall liner, head and piston were treated as constant surface temperature conditions, in which the temperature equals either the measured coolant temperature or the oil temperature in the crankshaft case.

This is reasonable because the variation of the temperature on these surfaces is much smaller than that on the inner surfaces of the combustion chamber. The boundary condition on the inner gas-side surface of the combustion chamber was a specified heat flux, which was obtained through the cycle simulation process.

The numerical method used here is the Crank-Nicolson method which is an implicit and accurate method. For the constant coefficient heat conduction equation, ($T_t = \alpha(T_{xx} + T_{yy})$) the Crank-Nicolson method is [4]:

$$\frac{u_{i,j}^{n+\frac{1}{2}} - u_{i,j}^{n}}{\frac{\Delta t}{2}} = a\ \frac{1}{2}\left[\frac{u_{i+1,j}^{n+\frac{1}{2}} - 2u_{i,j}^{n+\frac{1}{2}} + u_{i-1,j}^{n+\frac{1}{2}}}{(\Delta x)^2} + \frac{u_{i+1,j}^{n} - 2u_{i,j}^{n} + u_{i-1,j}^{n}}{(\Delta x)^2}\right] \quad (7)$$

$$\frac{u_{i,j}^{n+1} - u_{i,j}^{n+\frac{1}{2}}}{\frac{\Delta t}{2}} = a\ \frac{1}{2}\left[\frac{u_{i,j+1}^{n+1} - 2u_{i,j}^{n+1} + u_{i,j-1}^{n+1}}{(\Delta y)^2} + \frac{u_{i,j+1}^{n+\frac{1}{2}} - 2u_{i,j}^{n+\frac{1}{2}} + u_{i,j-1}^{n+\frac{1}{2}}}{(\Delta y)^2}\right] \quad (8)$$

Piston movement is a complicated feature that characterizes engine operation which is important in the heat conduction problem.

Assuming that the connecting rod length is *l*, crank radius is *r*and crank angle is θ, then according to Fig. 3(a) [5]:

$$s = r(1-\cos\theta) + l - (l^2 - r^2\sin^2\theta)^{\frac{1}{2}} \quad (9)$$

$$z_p = r\cos\theta + (l^2 - r^2\sin^2\theta)^{\frac{1}{2}} + b \quad (10)$$

$$v_p = 2\pi r N \sin\theta\left[1 + \frac{\cos\theta}{(l^2 - r^2\sin^2\theta)^{\frac{1}{2}}}\right] \quad (11)$$

Where s_c is the squish height; s is the piston position; z_p is the distance between the crank axis and the piston top surface; v_p is the instantaneous piston velocity; N is the rotational speed of the crankshaft and b is the distance between the piston top surface and the piston pin axis.

In this research a special technique was developed to solve the moving boundary problem of engine pistons.

The grids were formed in a cylindrically symmetric domain were the left side represent the centerline of the engine cylinder.

Nodes representing boundaries or inner points of the cylinder wall, head and piston were determined.

These nodes participate in the computation and are termed computed nodes, but others outside the boundaries are non-computed nodes. In Fig. 3 (b) the nodes in the white regions are the computed nodes and the nodes in shadowed regions are the non-computed nodes.

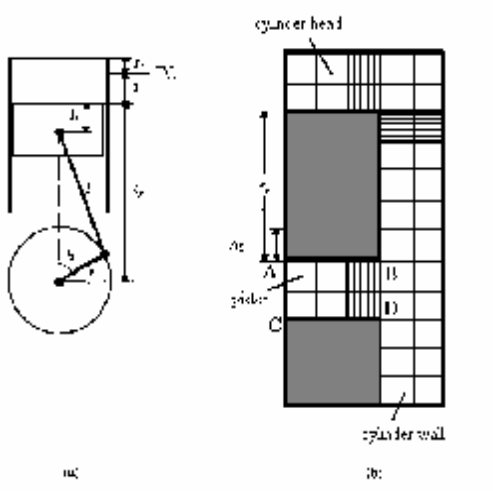

Fig. 3. Schematic Diagrams Showing;
(a) geometrical relation-ships of piston movement
(b) grid distribution in an engine cylinder

The computed nodes representing the piston and the gap between the piston and cylinder wall [region ABCD in Fig. 3 (b)] are separated from other computed nodes. When the engine is running, the piston position s is determined using eqn (9).

If $s+s_c$ is moved to $s_p - \Delta z$ in the next time step [Fig. 3(b)], the nodes just above the piston top boundary AB are converted into the nodes of a new top boundary and the nodes on the former bottom boundary CD are changed into non-computed nodes.

Meanwhile, temperatures at each node at the former piston position are moved to the corresponding node at the new piston position.

In this way the upward piston movement is realized in the finite difference analysis. Downward piston movement is treated with an analogous method.

Instead of a flat-topped piston such as that typically used in spark-ignition engines, Diesel engines usually have a piston with bowl.

In medium-to-small size direct-injection Diesel engines, use of a bowl-in-piston combustion chamber results in substantial swirl amplification at the end of the compression process. The effect of air swirl on the performance and emissions characteristic of this type of engine is very important.

In order to describe the configuration of a bowl-shaped piston in the finite difference representation, tabular information about the piston outline is used [i.e. the coordinates r_i and z_i in Figure 4.

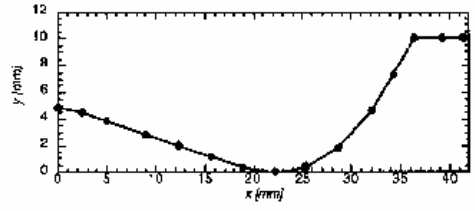

Fig. 4. Silhouette of Piston Bowl

The finite difference equations are most efficiently solved in a rectangular domain. Thus, it is convenient to transform the nonrectangular physical domain to a rectangular computational domain. From the geometry characteristics, the relationship between the physical and the computational domain can be defined as

$$\xi = \xi(r, z) = r \tag{12}$$

$$\eta = \eta(r, z) = z - \left[\frac{z_{i+1} - z_i}{r_{i+1} - r_i} (r - r_i) + z_i \right] \tag{13}$$

$$(r_i < r < r_{i+1})$$

Where $\xi = \xi(r, z)$ and $\eta = \eta(r, z)$ are mapping functions.

5. Results and Discussion

According to the engine specifications, a finite difference model of this engine was set up. Figure 5 shows the grids and boundary conditions of the model for the fine grid option. The grid number in the r-direction is 34 for the fine grid option, which includes four grids within the piston-liner air gap.

The grid size in the r-direction depends on the piston silhouette and the distribution of its outline points (it is 0.1 mm within the air gap, and 0.05, 0.1 or 1 mm with increasing depth below the cylinder wall). The grid number in the z-direction, however, is much more than that in the r-direction and it is 126 for the fine option. The grid size in z-direction is 1 mm within the cylinder wall and 0.05, 0.1, 0.2 or 2 mm with increasing depth below the head surface.

The gasket between the head liner and cylinder is made of a metal compressed material where its thermal resistance was neglected in this model. Piston rings and the gas between them occupy the gap between the piston and the cylinder wall.

In order to include the effects of piston rings on heat conduction, the piston ring properties for gap grids from the bottom of the piston to the fifth mesh point were given.

The temperatures above the head liner and outside the cylinder wall were designated as $T_{01} = 361K$ and $T_{02} = 361K$, i.e. the same as the coolant temperature; where the temperatures on the bottom surface of the piston and on the inner surface of the cylinder wall below the piston were specified as $T_{oil1} = 375K$ and $T_{oil2} = 368K$. For the fired case the corresponding temperatures are $T_{01} = 645K$, $T_{02} = 401K$, $T_{oil1} = 675K$, $T_{oil2} = 368K$, respectively.

The instantaneous temperature at a point located on the head liner surface has been measured for both motored and fired engine operation cases [6]. Based on the instantaneous surface temperature, the heat flux at this point was calculated using the transient heat conduction equation.

For the motored case, the calculation time step is $2.78\times10^{-5}s$ (i.e. 0.25 crank angle degrees) and for the fired case, the calculation time step is $2.76\times10^{-5}s$.

Figures 6 and 7 compare the computed and measured temperature at the monitoring point for the motored and fired cases. Note that, in this case the finite difference code was run for 500 engine cycles (starting from the uniform wall temperature initial condition of $T = 355K$) until a pseudo-steady state was reached (i.e. for the warmed up engine).

The computed temperature in the measurement position is in good agreement with the measured temperature for both the motored and fired cases. These results strongly verify that the present code developed in this study is suitable for modeling the temperature distribution of the combustion chamber surfaces in engines.

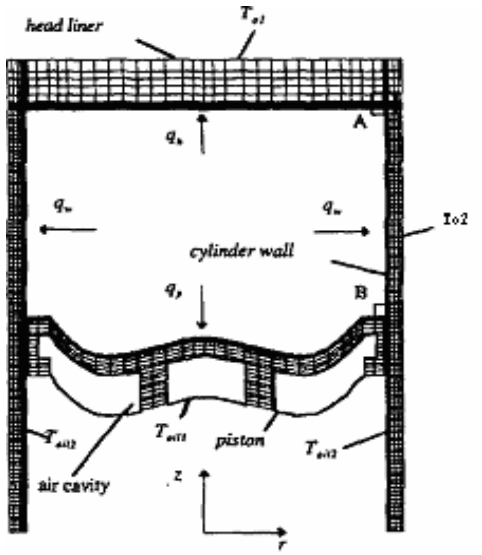

Fig. 5. Numerical Mesh of Isuzu Ceramic Diesel Engine at 90° ATDC

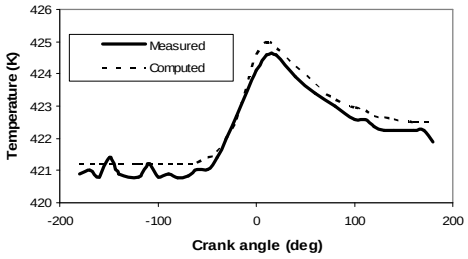

Fig. 6. Surface Temperature Ccomparison on the Cylinder Head for Motored Case

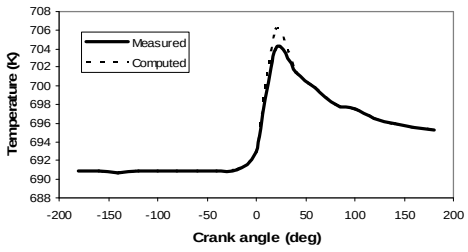

Fig. 7. Surface Temperature Comparison on the Cylinder Head for Fired Engine case

The computed time-averaged temperature distributions on each surface of the combustion chamber are shown in Fig. 8 to 10.

The temperature distributions for the cylinder head was shown in Fig. 8 which is 50-120 K lower than the original (assumed) constant temperature, and have their maximum value at the edge of the bowl. The maximum time-averaged temperature difference at points on the surface is about 70 K.

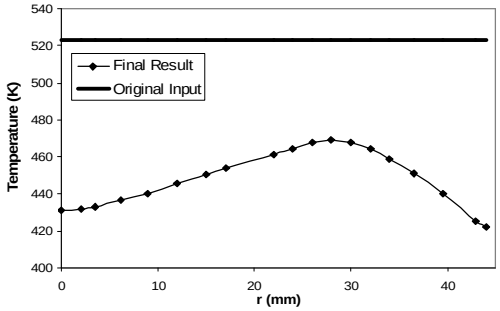

Fig. 8. Predicted Time-Averaged Temperature Distributions on the Cylinder Hhead Ssurface

Temperature distributions for the piston was given in Fig. 9 which is also lower than the original guess, which formed a high temperature region on the bowl-side surface and a low temperature region on the bowl-valley surface.

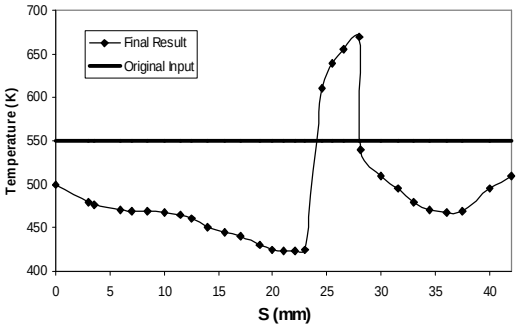

Fig. 9. Predicted Time-Averaged Temperature Distributions on the Piston Surface

Figure 10 shows that the temperature distributions on the cylinder wall surface is the same as the oil temperature adjacent to the wall for the majority of locations on the surface, but there is a 30 K increment in temperature in the region near the cylinder head.

This proves that combustion and heat transfer within the cylinder do not have much influence on the temperature distribution of the wall surface, except for in a narrow region in the ring reversal region near the cylinder head. A detailed presentation of the effect of combustion chamber mean wall temperature on engine performance, as calculated from the thermodynamic cycle simulation model, is given in figures 11 to 15. As expected, a considerable increase in the maximum gas temperature is observed, accompanied by a corresponding decrease of volumetric efficiency as the wall temperature increases [7].

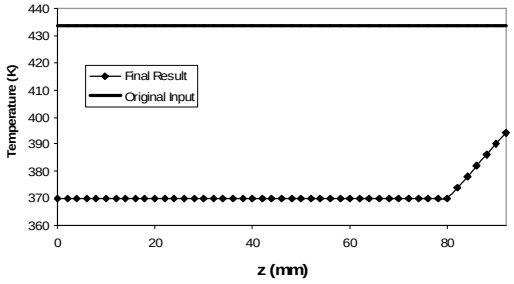

Fig. 10. Predicted time-Averaged Temperature Distributions on the Cylinder Liner Wall

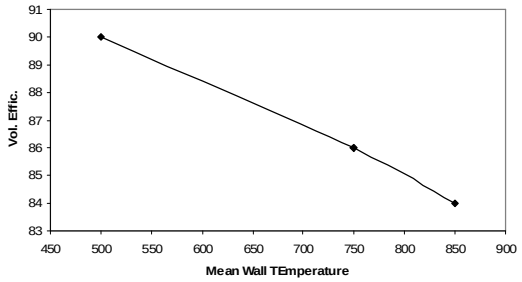

Fig. 11. Difference of Volumetric Efficiency Versus Mean Wall Temperature

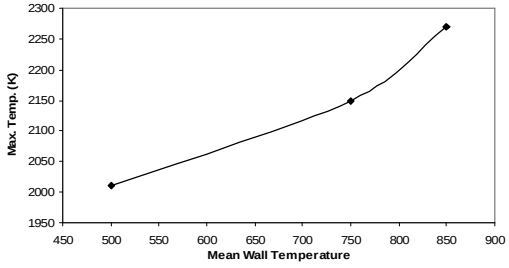

Fig. 12. Difference of maximum temperature versus mean wall temperature

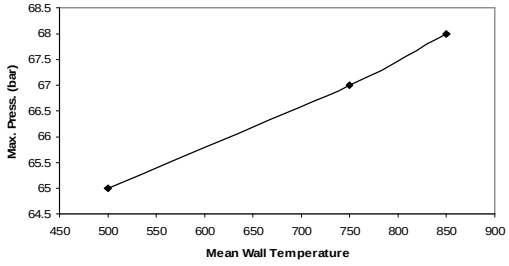

Fig. 13. Difference of Maximum Pressure Versus Mean Wall Temperature

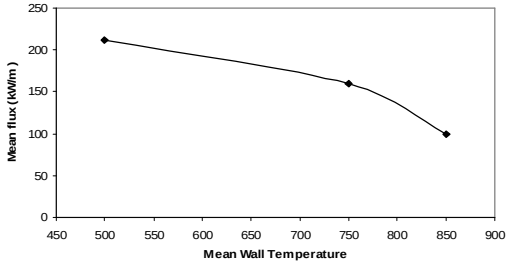

Fig. 14. Difference of Average heat Flux Versus Mean Wall Temperature

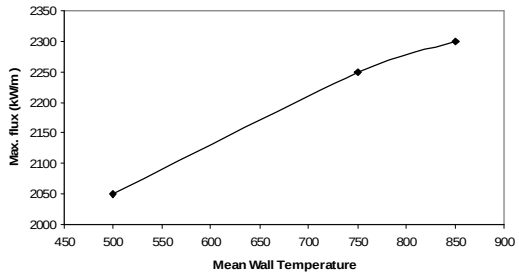

Fig. 15. Difference of Maximum Heat Flux Versus Mean Wwall temperature

The average amount of heat flux to the wall present a significant decrease as the wall temperature increases, whereas the corresponding peak heat flux increases. This is mainly due to the fact that the increased cylinder surface temperature causes a respective increase in the peak value of convective heat transfer coefficient, and so the expected gain from the reduction of heat losses (due to the elevated wall surface temperatures) almost vanishes or is even reversed over a certain part of the engine cycle.

6. Conclusion

The cylinder working fluid mean temperature, rate of heat fluxes to combustion chamber and temperature distribution on combustion chamber surface were successfully developed in this study. The numerical method used is Crank-Nicolson finite difference method. This method is characterized by its implicit nature, unconditional numerical stability and good accuracy.

Special treatments for the head gasket and the piston-liner air gap, and a grid transformation for describing the realistic piston bowl shape were designed and utilized in the present study. The accomplishment of modeling piston movement within the present finite difference formulation makes this code a computer program with the capability of realistic engine simulation.

This code was used to calculate heat conduction processes occurring in the combustion chambers of an Isuzu ceramic engine. The present code provides an accurate and consistent method for obtaining the temperature distributions within engine components and these results would also be useful for structural analysis.

References

[1] Borman, G.L. and Nishiwaki, K., *"Internal combustion engine heat transfer*". Progress in Energy Combustion Science, 1987, 13**,** 1-46.

[2] Amsden, A.A., O'Rourke, P.J., and Butler, T.D., KIVA-II*: "A Computer Program for Chemically Reactive Flows with Sprays"*. Los Alamos National Labs, LA-11560-MS, 1989.

[3] Ferguson, Colin R., "*Internal Combustion Engines-Applied Thermosciences*", John Wiley & Sons, New York, 1986.

[4] Hoffmann, Klaus A., Chiang, Steve T., *"Computational fluid dynamics for engineers"*, McGraw-Hill, New York, 1995.

[5] Heywood, J.B., *"Internal Combustion Engine Fundamentals"*. McGraw-Hill, New York, 1989.

[6] Simescu, S., "*Heat flux measurements of the combustion chamber head surface of a silicon nitride D.I. Diesel engine*". Ph.D. thesis, University of Wisconsin-Madison, 1997.

[7] Rakopoulos, C.D., Andritsakis, E.C., and Hountalas, D. T., "*The influence of the exhaust system unsteady gas flow and insulation on the performance of a multi-cylinder turbocharged diesel engine", Heal Recovery Systems & CHP*15, 51-72, 1995.